*mathematics*

MDPI

*Article*

# Relaxed Stabilization Criteria for Polynomial Fuzzy Systems via Switched Fuzzy Controller

**Mohan Hao and Lantian Guo ***

School of Automation and Electronic Engineering, Qingdao University of Science and Technology, Qingdao 266061, China; haomohanwf@hotmail.com
* Correspondence: lantianguo@qust.edu.cn

**Abstract**

This paper studies the problem of controller design for polynomial fuzzy-model-based (PFMB) systems. To make full use of the information of membership functions (MFs), the operating space is partitioned into several subspaces. According to the information of partitions, switched state feedback and output feedback controllers are designed, respectively, for the system. By employing the approximated membership function method and a new relaxation technique, relaxed stabilization criteria in the form of the sum of squares are derived without the need to impose any constraints on system matrices. Simulation examples are provided to illustrate the validity of the presented method.

**Keywords:** polynomial fuzzy-model-based system; sum of squares; stabilization; switched fuzzy controller

**MSC:** 93C10; 93D09; 93D15

## 1. Introduction

Nonlinearity is a common phenomenon in practical systems, and the analysis and synthesis of such systems are both challenging and important. T-S fuzzy models, which combine several simple linear subsystems according to membership functions, can describe a large class of complex real-world systems [1–3]. In the past few decades, extensive studies have been conducted on T-S fuzzy systems [4–8]. The quadratic Lyapunov design method is a basic and important method for deriving stability and stabilization criteria [2,9–14]. However, this design has not made full use of the important information of MFs. In addition, under the quadratic Lyapunov method, the rules and premise MFs of fuzzy controllers must be consistent with those of the fuzzy systems, which constrains the flexibility of controller design. By utilizing the information of MFs, various relaxed stability and stabilization conditions are obtained [15–20]. Moreover, some results allow the fuzzy systems and controllers to not need to share the same rules and MFs [17,18,21,22].

In the last few years, the PFMB system [23–25] has attracted increasing attention because it can better describe nonlinear systems [9]. An SOS technique has been developed to analyze and control PFMB systems. The work in [17] provides a novel idea that breaks through the long-standing barrier in stability analysis by bringing the membership functions into the stability analysis, leading to membership-function-dependent conditions for the first time. In addition, the novel concept of imperfect premise-matching design proposed in [18], which allows the number of rules and/or premise membership functions of the fuzzy controller to differ from those of the fuzzy model, is extended to the

Check for updates

Academic Editor: Cheng-Hung Huang

Received: 7 May 2026
Revised: 2 June 2026
Accepted: 8 June 2026
Published: 10 June 2026

**Copyright:** © 2026 by the authors. Licensee MDPI, Basel, Switzerland. This article is an open access article distributed under the terms and conditions of the Creative Commons Attribution (CC BY) license.

stability analysis of positive PFMB control systems [26], output regulation [22], output feedback tracking control [21,27,28], sampled-data output feedback stabilization [29] for PFMB systems, and interval type-2 polynomial fuzzy-model-based control for networked control systems [24]. These methods make good use of the information of MFs, and the conservatism of stability conditions can be reduced. For the problem of output feedback control, the SOS-based conditions are usually obtained by using a Lyapunov matrix with special structures, which is a source of conservatism.

Switched dynamical systems are composed of a collection of subsystems together with a switching rule that specifies the switching among the subsystems [20,30,31]. If a single controller cannot achieve the control purpose, a switched controller can be considered. For fuzzy systems, a single fuzzy controller design may bring much conservatism [32,33]. In [34], the authors partition the operating space into two kinds of subregions, namely crisp regions and fuzzy regions, and design the piecewise affine controller for the continuous-time fuzzy systems. In [23], a switching polynomial fuzzy control scheme was proposed that makes use of regional membership function information and switching Lyapunov function to facilitate stability analysis and control synthesis. In [35,36], more advanced switching polynomial fuzzy control schemes and analysis were proposed. To date, research still focuses on reducing the conservatism of stability and stabilization conditions.

In this paper, we present a switched control scheme for PFMB systems via state and static output feedback control. We partition the operating space of MFs into several subspaces according to their values. The controllers are designed so that they switch when the subregion changes from one to another. By employing the approximated membership function technique and the new relaxation method, convex stabilization conditions are derived in the form of SOS. As demonstrated in the numerical examples, the design of switched controllers and the introduction of the new relaxation method play an important role in reducing the conservatism of the stabilization criteria.

The main contributions of this paper are threefold: (i) A unified switched fuzzy control framework that encompasses both state feedback and static output feedback designs for PFMB systems, where the operating space is partitioned based on membership function information to enable subspace-dependent controller gains. (ii) The removal of the structural constraint on the Lyapunov matrix in the SOF design, which is a key source of conservatism in [29], enabled by the new relaxation technique and a congruence transformation argument. Compared with the method in [23], which also employs switching polynomial fuzzy control, our approach differs in that our switching rule is based on a simpler MF partition that is easier to implement. Compared with the methods in [35,36], which employ more advanced switching schemes, our approach achieves a favorable trade-off between conservatism reduction and computational efficiency.

*Notation*: Throughout this paper, the underlying notations are standard. In particular, $B = diag\{A_1, A_2, \ldots, A_n\}$ denotes that the matrix $B$ is a diagonal matrix whose diagonal elements are $A_1, \ldots, A_n$. For one matrix $A$, $Sym\{A\}$ means that $Sym\{A\} = A + A^T$, $A^{-T}$ represents $(A^{-1})^T$.

## 2. Problem Formulation

In this section, an $r$-rule PFMB model is described as follows:

$$\begin{cases} \dot{x}(t) = \sum_{i=1}^{r} w_i(\theta(t))(A_i(x(t))x(t) + B_i(x(t))u(t)), \\ y(t) = \sum_{i=1}^{r} w_i(\theta(t))C_i(x(t))x(t), \end{cases} \tag{1}$$

where $x(t) \in \mathbb{R}^n$ is the system state, $u(t) \in \mathbb{R}^m$ is the control input, and $y(t) \in \mathbb{R}^p$ is the measured output vector. $A_i(x(t)) \in \mathbb{R}^{n\times n}$, $B_i(x(t)) \in \mathbb{R}^{n\times m}$, $C_i(x(t)) \in \mathbb{R}^{p\times n}$ are the

known polynomial matrices in $x(t)$ with appropriate dimensions. The polynomial entries of $A_i$, $B_i$, and $C_i$ allow the PFMB model to exactly represent polynomial nonlinear systems within the operating region, which is more general than T-S fuzzy models with constant system matrices. $w_i(\theta(t))$, $i = 1, 2, .., r$, are the normalized MFs with the characteristics of $w_i(\theta(t)) \geq 0$ for all $i$, and $\sum_{i=1}^{r} w_i(\theta(t)) = 1$.

The premise variable $\theta(t)$ captures the nonlinearity of the system and determines the activation of each fuzzy rule through the membership functions $w_i(\theta(t))$. It is typically chosen as state components or functions thereof (e.g., $\theta(t) = x_1(t)$ in the simulation examples). Throughout the paper, the function $\theta(t)$ is assumed to be measurable. This measurability assumption (Assumption 1) is necessary for determining the active subspace and implementing the switching rule in the controller.

The fuzzy model (1) is transformed into a switched one according to the MF partition. Taking the characteristics of the MFs into consideration, the operating space $\theta(t) \in [\underline{\theta}, \overline{\theta}]$ of MFs is divided into $q$ subspaces $\underline{\theta} = \theta_0 \leq \theta_1 \leq \theta_2 \leq \cdots \leq \theta_{q-1} \leq \theta_q = \overline{\theta}$.

Based on the partition, the $s$-rule state and static output feedback (SOF) controllers are employed to control the systems. The state feedback controller is designed as follows:

$$u(t) = \sum_{j=1}^{s} m_j(\theta(t)) K_{jr_t}(x(t)) x(t), \tag{2}$$

where the process $r_t$, $t \geq 0$, taking values in a finite set $S = 1, 2, \ldots, q$, governs the switching among different controller modes with

$$\begin{aligned} r_{t+\Delta} = \bar{j} | r_t = \bar{i}, \qquad & \textit{if and only if } \theta(t) \in [\theta_{\bar{i}-1}, \theta_{\bar{i}}], \\ & \textit{and } \theta(t+\Delta) \in [\theta_{\bar{j}-1}, \theta_{\bar{j}}]. \end{aligned} \tag{3}$$

$K_{jr_t}(x(t))$, $m_j(\theta(t))$, $j = 1, 2, \ldots, s$, respectively, are the switched controller gains, the normalized MFs of the controller with the characteristics of $m_j(\theta(t)) \geq 0$ for all $j$, and $\sum_{j=1}^{s} m_j(\theta(t)) = 1$.

The switched SOF controller is given as

$$\begin{aligned} u(t) &= \sum_{j=1}^{s} m_j(\theta(t)) Y_{jr_t}(x(t)) (\sum_{j=1}^{s} m_j(\theta(t)) Z_{jr_t}(x(t)))^{-1} \bar{y}(t), \\ &= \sum_{j=1}^{s} \sum_{k=1}^{r} m_j(\theta(t)) w_k(\theta(t)) Y_{jr_t}(x(t) (\sum_{j=1}^{s} m_j(\theta(t)) Z_{jr_t}(x(t)))^{-1} \bar{C}_k(x(t)) x(t), \end{aligned} \tag{4}$$

where $\bar{y}(t) = \begin{bmatrix} y(t) \\ 0_{1\times(n-p)} \end{bmatrix}$, $\bar{C}_k(x(t)) = \begin{bmatrix} C_k(x(t)) \\ 0_{(n-p)\times n)} \end{bmatrix}$, $Y_{jr_t}(x(t))$ and $Z_{ir_t}(x(t))$ are the polynomial matrices to be solved.

Combining (1) and (2), we obtain the switched fuzzy system with the state feedback controller as

$$\dot{x}(t) = \sum_{i=1}^{r} \sum_{j=1}^{s} w_i(\theta(t)) m_j(\theta(t)) (A_i(x(t)) + B_i(x(t)) K_{jr_t}(x(t))) x(t). \tag{5}$$

Substituting (4) into (1), we obtain that

$$\begin{aligned} \dot{x}(t) = & \sum_{i=1}^{r} \sum_{j=1}^{s} \sum_{k=1}^{r} w_i(\theta(t)) m_j(\theta(t)) w_k(\theta(t)) (A_i(x(t)) \\ & + B_i(x(t)) Y_{jr_t}(x(t)) (\sum_{j=1}^{s} m_j(\theta(t)) Z_{jr_t}(x(t)))^{-1} \bar{C}_k(x(t))) x(t). \end{aligned} \tag{6}$$

**Remark 1.** *According to the information of MFs, the operating space $\theta(t)$ is partitioned into several subspaces. In each subspace, the linear subsystems of fuzzy systems have different weights. Hence, the fuzzy system has different local features in different subspaces. By partition, the fuzzy system can be regarded as a switched fuzzy system together with a switching rule (3). The method of designing a switched fuzzy controller for a switched fuzzy system takes better account of the local characteristics of fuzzy systems than existing methods.*

**Remark 2.** *In practice, signal errors of $\theta(t)$ may be produced with the influence of noises, delay, and measuring errors. To ensure accuracy, the subspaces can overlap each other as $\underline{\theta} = \underline{\theta}_1 < \underline{\theta}_2 \leq \cdots < \underline{\theta}_i \leq \bar{\theta}_{i-1} < \underline{\theta}_{i+1} \leq \bar{\theta}_i < \cdots < \bar{\theta}_q = \bar{\theta}$, and the switching rule is designed as $r_{t+\Delta} = j | r_t = i$, if and only if $\theta(t) \in [\underline{\theta}_i, \bar{\theta}_i]$, and $\theta(t+\Delta) \in [\frac{\underline{\theta}_j + \bar{\theta}_{j-1}}{2}, \frac{\bar{\theta}_j + \underline{\theta}_{j+1}}{2}]$.*

## 3. Stabilization Criteria

In this section, we will design the switched controllers for system (1) by using the approximated membership function method. In the following, the time $t$ associated with the variables is dropped for brevity, e.g., $x(t)$ and $\theta(t)$ are denoted as $x$ and $\theta$, respectively. The following lemma is useful in the proof of our main results [18].

**Lemma 1.** *Let $w_i^{\{\mu\}}$, $\mu = 1, 2, \ldots, l$ and $m_j^{\{\nu\}}$, $\nu = 1, 2, \ldots, \iota$, denote the sample points of MFs $w_i(\theta)$ and $m_j(\theta)$, respectively. $\bar{w}_i$ and $\bar{m}_j$ be the piecewise-linear MFs, which are used to approximate $w_i(\theta)$ and $m_j(\theta)$, respectively. The condition*

$$\sum_{i=1}^{r} \sum_{j=1}^{s} w_i(\theta) m_j(\theta) \Theta_{ij} < 0, \tag{7}$$

*can be solved by the following conditions:*

$$\begin{aligned} &-\vartheta^T \Big(\sum_{i=1}^{r} \sum_{j=1}^{s} (w_i^{\{\mu\}} m_j^{\{\nu\}} + \gamma_{ij}) \Theta_{ij} + \gamma_{ij} M(x) + \varepsilon_1(x) I\Big) \vartheta \text{ are SOS}, \ \forall \mu, \nu, \\ &-\vartheta^T (\Theta_{ij} + M(x) + \varepsilon_2(x) I) \vartheta \text{ are SOS}, \ \forall i, j, \end{aligned} \tag{8}$$

*where $w_i(\theta) m_j(\theta) - \bar{w}_i \bar{m}_j - \gamma_{ij} \geq 0$, $\varepsilon_1(x)$ and $\varepsilon_2(x)$ are predefined scalar polynomials, and $M(x)$ is a polynomial matrix to be determined.*

Next, the boundary points in $[\underline{\theta}, \bar{\theta}]$ of the membership function partition are chosen among the abscissa of those sample points $w_i^{\{\mu\}}$ and $m_j^{\{\nu\}}$ unless noted otherwise.

### 3.1. State Feedback Controller Design

**Theorem 1.** *The closed-loop PFMB system (5) is asymptotically stable, if there exist polynomial matrices $Q(x)$, $M_{r_t}(x)$, $Y_{jr_t}(x)$, such that the following conditions hold:*

$$\begin{aligned} &\vartheta^T (Q(x) - \varepsilon_1(x) I) \vartheta \text{ is SOS}, \\ &-\vartheta^T (\Phi_{ijr_t} + M_{r_t}(x) + \varepsilon_2(x) I) \vartheta \text{ are SOS}, \ \forall i, j, r_t, \\ &-\vartheta^T \Big(\sum_{i=1}^{r} \sum_{j=1}^{s} (w_{ir_t}^{\{\mu\}} m_{jr_t}^{\{\nu\}} + \gamma_{ijr_t}) \Phi_{ijr_t} + \gamma_{ijr_t} M_{r_t}(x) + \varepsilon_3(x) I\Big) \vartheta \text{ are SOS}, \ \forall \mu, \nu, k, \end{aligned} \tag{9}$$

*where $\Phi_{ijr_t} = Sym\{A_i(x) Q(x) + B_i(x) Y_{jr_t}\} - \sum_{\kappa \in \mathbf{K}} \frac{\partial Q(x)}{\partial x_\kappa} A_i^\kappa(x) x$, where $A_i^\kappa(x)$, and $B_i^\kappa(x)$, $i = 1, 2, \ldots, r$, $\kappa = 1, 2, \ldots, n$, denote the $\kappa$th row of $A_i(x)$ and $B_i(x)$, respectively, [18]. $w_{ir_t}(\theta) m_{jr_t}(\theta) - \bar{w}_{ir_t} \bar{m}_{jr_t} - \gamma_{ijr_t} \geq 0$, $w_{ir_t}^{\{\mu\}}$, $m_{jr_t}^{\{\nu\}}$, $w_{ir_t}(\theta)$, $m_{jr_t}(\theta)$, $\bar{w}_{ir_t}$, and $\bar{m}_{jr_t}$, respectively,*

*represent the sample points* $w_i^{\{\mu\}}$, $m_j^{\{\nu\}}$, *the MFs* $w_i(\theta)$, $m_j(\theta)$, *and the piecewise-linear MFs* $\bar{w}_i$, $\bar{m}_j$ *in* $[\theta_{\bar{i}-1}, \theta_{\bar{i}}]$, *if* $r_t = \bar{i}$. $\vartheta \in \mathbb{R}^n$ *is an arbitrary vector independent of* $x(t)$. $\varepsilon_i(x)$, $i = 1, 2, 3$, *are prescribed polynomial scalars. If this is the case, the state feedback controller gains can be solved by* $K_{jr_t}(x) = Y_{jr_t}(x)Q^{-1}(x)$, $r_t = 1, 2, \ldots, q$.

**Proof.** By Lemma 1, the conditions in (9) can ensure that

$$\sum_{i=1}^{r}\sum_{j=1}^{s} w_i(\theta)m_j(\theta)\Phi_{ijr_t} < 0. \tag{10}$$

We now show that this implies the asymptotic stability of the closed-loop system. Pre- and postmultiplying the left and right sides of (10) by $Q^{-1}(x)$, respectively, we obtain that

$$\sum_{i=1}^{r}\sum_{j=1}^{s} w_i(\theta)m_j(\theta)(Sym\{Q^{-1}(x)A_i(x) + Q^{-1}(x)B_i(x)K_{jr_t}\} + \dot{Q}^{-1}(x)) < 0, \tag{11}$$

where we have used the identity $\dot{Q}^{-1}(x) = -Q^{-1}(x)\dot{Q}(x)Q^{-1}(x)$ and the definition $\Phi_{ijr_t} = Sym\{A_i(x)Q(x) + B_i(x)Y_{jr_t}\} - \sum_\kappa \frac{\partial Q}{\partial x_\kappa}A_i^\kappa x$, with $K_{jr_t}(x) = Y_{jr_t}(x)Q^{-1}(x)$. The term $\sum_\kappa \frac{\partial Q}{\partial x_\kappa}A_i^\kappa x$ arises from the time derivative of the state-dependent Lyapunov matrix $Q^{-1}(x)$ using the chain rule: $\dot{Q}^{-1}(x) = \sum_{\kappa=1}^{n}\frac{\partial Q^{-1}(x)}{\partial x_\kappa}\dot{x}_\kappa$. which implies that the polynomial Lyapunov function satisfies

$$\begin{aligned} V(t) &= x^T Q^{-1}(x)x > 0, \\ \dot{V}(t) &= \sum_{i=1}^{r}\sum_{j=1}^{s} w_i(\theta)m_j(\theta)x^T(Sym\{Q^{-1}(x)A_i(x) \\ &\quad + Q^{-1}(x)B_i(x)K_{jr_t}\} + \dot{Q}^{-1}(x))x < 0. \end{aligned} \tag{12}$$

Since $V(t) > 0$ and $\dot{V}(t) < 0$ hold for all $x \neq 0$ and all $t \geq 0$, by the Lyapunov stability theorem, the equilibrium $x = 0$ of the closed-loop system (5) is asymptically stable. The proof is completed. □

**Remark 3.** *In Theorem 1, the approximated membership function technique is used. In each subspace of* $\theta(t)$, *the MFs have different local characteristics, which leads to system differences in different subspaces. The method to design switched fuzzy controllers can effectively reduce the conservatism, which is illustrated by simulation examples in the following section.*

### *3.2. Static Output Feedback Controller Design*

**Theorem 2.** *The closed-loop PFMB system (6) is asymptotically stable if there exist polynomial matrices* $Q(x)$, $M_{r_t}(x)$, $Y_{jr_t}(x)$, $Z_{jr_t}$, *such that the following conditions hold:*

$$\begin{aligned} &\vartheta_1^T(Q(x) - \varepsilon_1(x)I)\vartheta_1 \ \ is \ \ SOS, \\ &-\vartheta^T(P_{ijr_t} + M_{r_t}(x) + \varepsilon_2(x)I)\vartheta \ \ are \ \ SOS, \ \forall\, i, j, r_t, \\ &-\vartheta^T(\sum_{i=1}^{r}\sum_{j=1}^{s}(w_{ir_t}^{\{\mu\}}m_{jr_t}^{\{\nu\}} + \gamma_{ijr_t})P_{ijr_t} + \gamma_{ijr_t}M_{r_t}(x) + \varepsilon_3(x)I)\vartheta \ \ are \ \ SOS, \ \forall\, \mu, \nu, r_t, \end{aligned} \tag{13}$$

*where* $P_{ijr_t} = \begin{bmatrix} \Phi_{ijr_t} & \beta(B_i(x)Y_{jr_t}(x)) + (\bar{C}_i(x)Q(x) - Z_{jr_t}(x))^T \\ * & -\beta Z_{jr_t}(x) - \beta Z_{jr_t}^T(x) \end{bmatrix}$, *and* $\Phi_{ijr_t}$, $\gamma_{ijr_t}$, $w_{ir_t}^{\{\mu\}}$, $m_{jr_t}^{\{\nu\}}$ *are defined in Theorem 1.* $\vartheta_1 \in \mathbb{R}^n$, $\vartheta \in \mathbb{R}^{2n}$ *are arbitrary vectors independent of* $x(t)$. $\beta$ *and* $\varepsilon_i(x)$, $i = 1, 2, 3$, *are prescribed polynomial scalars.*

**Proof.** According to Lemma 1, the conditions in (13) imply that

$$\sum_{i=1}^{r}\sum_{j=1}^{s} w_i(\theta)m_j(\theta)P_{ijr_t} < 0. \tag{14}$$

Pre- and postmultiplying the left and right sides of (14) by $diag\{Q^{-1}(x), \frac{1}{\beta}Q^{-1}(x)\}$, respectively, leads to inequality (15),

$$\begin{aligned}
&\sum_{i=1}^{r}\sum_{j=1}^{s} w_i(\theta)m_j(\theta)\begin{bmatrix} Sym\{Q^{-1}(x)A_i(x) + Q^{-1}(x)B_i(x)\bar{Y}_{jr_t}\} + \dot{Q}^{-1}(x) & * \\ (Q^{-1}(x)B_i(x)\bar{Y}_{jr_t}(x))^T + \frac{1}{\beta}(Q^{-1}(x)\bar{C}_i(x) - \bar{Z}_{jr_t}(x)) & -\frac{1}{\beta}\bar{Z}_{jr_t}(x) - \frac{1}{\beta}\bar{Z}_{jr_t}^T(x) \end{bmatrix} \\
= &\sum_{i=1}^{r}\sum_{j=1}^{s} w_i(\theta)m_j(\theta)\begin{bmatrix} Sym\{Q^{-1}(x)A_i(x) + Q^{-1}(x)B_i(x)\bar{Y}_{jr_t}\} + \dot{Q}^{-1}(x) & * \\ (Q^{-1}(x)B_i(x)\bar{Y}_{jr_t}(x))^T & 0 \end{bmatrix} \\
&+\sum_{i=1}^{r} w_i(\theta)Sym\left\{\begin{bmatrix} 0 \\ I \end{bmatrix}\frac{1}{\beta}\mathbf{Z}\begin{bmatrix} (\mathbf{Z}^{-1}Q^{-1}(x)\bar{C}_i(x) - I) & -I \end{bmatrix}\right\} \\
&< 0.
\end{aligned} \tag{15}$$

where $\bar{Y}_{jr_t}(x) = Y_{jr_t}(x)Q^{-1}(x)$, $\bar{Z}_{jr_t}(x) = Q^{-1}(x)Z_{jr_t}(x)Q^{-1}(x)$, and $\mathbf{Z} = \sum_{j=1}^{s} m_j(\theta)\bar{Z}_{jr_t}(x)$.

Then, premultiplying (15) by the matrix $[I \;\; (\mathbf{Z}^{-1}Q^{-1}(x)\bar{C}_i(x) - I)^T]$ and postmultiplying by its transpose, we obtain that

$$\begin{aligned}
&\sum_{i=1}^{r}\sum_{j=1}^{s}\sum_{k=1}^{r} w_i(\theta)m_j(\theta)w_k(\theta)Sym\{Q^{-1}(x)A_i(x) \\
&+Q^{-1}(x)B_i(x)Y_{jr_t}(\sum_{i=1}^{r} w_i(\theta)Z_{ir_t}(x))^{-1}\bar{C}_k(x)\} + \dot{Q}^{-1}(x) < 0,
\end{aligned} \tag{16}$$

which implies that $V(x) = x(t)^TQ^{-1}(x)x(t) > 0$, and $\dot{V}(x) = Sym\{\dot{x}^T(t)Q^{-1}(x)x(t)\} + x(t)^T\dot{Q}^{-1}(x)x(t) < 0$. The last inequality follows because the (2,2)-block of (15) vanishes after the congruence transformation with $[I \;\; (\mathbf{Z}^{-1}Q^{-1}(x)\bar{C}_i(x) - I)^T]$, and the resulting condition matches the closed-loop system dynamics (6). Since $V(x) > 0$ and $\dot{V}(x) < 0$, the closed-loop system is asymptotically stable by the Lyapunov stability theorem. This completes the proof. □

**Remark 4.** *The static output feedback problem is likely to cause NP-hard stability conditions. In Theorem 2, a new relaxation technique is used and the NP-hard condition is transformed into a new SOS-based one. Because a more general structure of Lyapunov matrix is introduced, the conservatism is reduced.*

### *3.3. Computational Complexity*

The computational complexity of the SOS-based stabilization conditions is determined by the size of the resulting SDP problem. For Theorem 1, the number of decision variables scales as $O(n^2d_Q^2 + rsqn^2d_Y^2)$, where $d_Q = \deg(Q(x))$ and $d_Y = \deg(Y_{jr_t}(x))$ are the polynomial degrees, and $q$ is the number of subspaces. The number of SOS constraints is $O(rsq + l\iota q)$, where $l$ and $\iota$ are the numbers of sample points for $w_i$ and $m_j$, respectively. For Theorem 2, the SDP size is further increased due to the enlarged matrix dimension $2n$ in $P_{ijr_t}$.

### *3.4. Guidelines for Parameter Selection*

The following practical guidelines are provided for selecting the key design parameters:

The partition points should be chosen at the boundaries where the membership functions exhibit significant changes, such as inflection points or crossover points where $w_i(\theta) = w_j(\theta)$. For systems with sigmoid-type MFs, partitioning at the mean value of the premise variable is a natural choice. Increasing the number of subspaces $q$ generally reduces conservatism but increases the number of SOS conditions. A practical approach is to start with $q = 2$ and increase until no further feasible region enlargement is observed.

More sample points provide tighter MF approximations (smaller approximation errors $\gamma_{ijr_t}$) and thus less conservative conditions, but they increase the SDP problem size. A practical strategy is to start with coarse sampling (e.g., integer-spaced points) and refine adaptively (e.g., half-integer spacing) until the feasible region converges.

Higher degrees for $Q(x)$ and $Y_{jr_t}(x)$ enlarge the feasible region at the cost of increased computation. The recommendation is to start with $\deg(Q) = 0$ and $\deg(Y) = 0$, and incrementally increase until no further improvement in the feasible region is observed.

The prescribed scalar polynomials $\varepsilon_i(x)$ should be chosen as small positive constants (e.g., $10^{-6}$) to ensure strict negativity of the SOS conditions. The scalar $\beta$ in Theorem 2 can be initialized as $\beta = 1$ and tuned to maximize the feasible region.

## 4. Simulation Examples

### *4.1. Example 1*

Consider the PFMB system (1) with three local models, and the system matrices are [18]:

$$A_1 = \begin{bmatrix} 1.59 - 0.12x_1^2 & -7.29 - 0.25x_1 \\ 0.01 & -0.1 \end{bmatrix},$$
$$A_2 = \begin{bmatrix} 0.02 - 0.63x_1^2 & -4.64 + 0.92x_1 \\ 0.35 & -0.21 \end{bmatrix},$$

$$A_3 = \begin{bmatrix} -a + 0.31x_1 - 1.12x_1^2 & -4.33 \\ 0 & 0.05 \end{bmatrix},$$
$$B_1 = \begin{bmatrix} 1 - 0.25x_1 + x_1^2 \\ 0 \end{bmatrix}, \; B_2 = \begin{bmatrix} 8 + 0.38x_1 \\ 0 \end{bmatrix},$$
$$B_3 = \begin{bmatrix} -b + 6 + x_1^2 \\ -1 \end{bmatrix},$$

where $a$ and $b$ are constant parameters.

The MFs of the system are chosen as

$$\begin{aligned} w_1(x_1) &= 1 - \frac{1}{1 + e^{-(x_1+4)}}, \\ w_3(x_1) &= \frac{1}{1 + e^{-(x_1-4)}}, \\ w_2(x_1) &= 1 - w_1(x_1) - w_3(x_1). \end{aligned}$$

The MFs of the fuzzy controller are given as

$$\begin{aligned} m_1(x_1) &= \begin{cases} 1, & for\ x_1 < -10, \\ \dfrac{-x_1+10}{20}, & for\ -10 \le x_1 \le 10, \\ 0, & for\ x_1 > 10, \end{cases} \\ m_2(x_1) &= 1 - m_1(x_1), \end{aligned}$$

which are straight lines. The operating space $x_1$ of MFs is partitioned into four subspaces as $(-\infty, -4]$, $[-4, 0]$, $[0, 4]$, and $[4, +\infty)$, which is depicted in Figure 1.

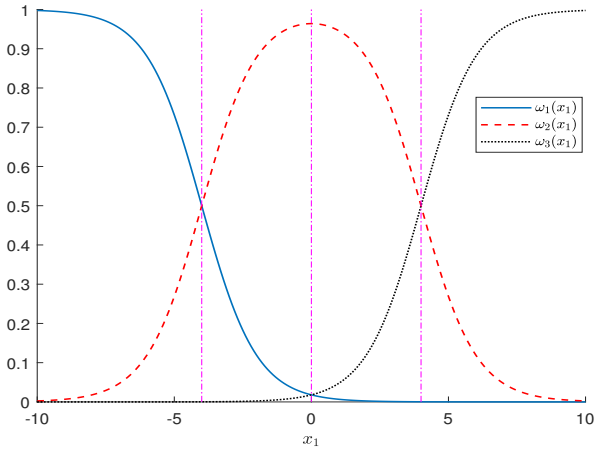



**Figure 1.** Membership function partition of Example 1.

The switched state feedback controller with two fuzzy rules is employed by Theorem 1 to stabilize the fuzzy system. The abscissa values of the sample points are chosen as $x_1 = \{-10, -9, \ldots, 9, 10\}$. It can be found numerically that

$$\begin{aligned} &If\ r_t = 1, Then \\ &\gamma_{11r_t} = 0, \gamma_{12r_t} = 0, \gamma_{21r_t} = -0.0090, \gamma_{22r_t} = -0.0026, \\ &\gamma_{31r_t} = -7.7866 \times 10^{-4}, \gamma_{32r_t} = -1.9966 \times 10^{-5}, \\ &If\ r_t = 2, Then \\ &\gamma_{11r_t} = -0.0073, \gamma_{12r_t} = -0.0044, \gamma_{21r_t} = 0, \gamma_{22r_t} = 0, \\ &\gamma_{31r_t} = -7 \times 10^{-5}, \gamma_{32r_t} = -1.9966 \times 10^{-5}, \\ &If\ r_t = 3, Then \\ &\gamma_{11r_t} = -7 \times 10^{-5}, \gamma_{12r_t} = -7 \times 10^{-5}, \gamma_{21r_t} = 0, \gamma_{22r_t} = 0, \\ &\gamma_{31r_t} = -0.0073, \gamma_{32r_t} = -0.0044, \\ &If\ r_t = 4, Then \\ &\gamma_{11r_t} = -7.7866 \times 10^{-4}, \gamma_{12r_t} = -1.9966 \times 10^{-5}, \\ &\gamma_{21r_t} = -0.0090, \gamma_{22r_t} = -0.0026, \\ &\gamma_{31r_t} = 0, \gamma_{32r_t} = 0. \end{aligned}$$

We set polynomial matrices $M(x_1)$ of degree 4, $Q$ of degree 0. The solutions of controller gains are found numerically by Theorem 1. Considering $Y_{jr_t}(x_1)$ of degrees 0 and 2, the feasible regions indicated by "•" and "○", respectively, are shown in Figure 2.

To illustrate the effectiveness of the method and for better comparison, we consider the sample points of $w_i(x_1)m_j(x_1)$ at $x_1 = \{-10, -9.5, -9, \ldots, 9, 9.5, 10\}$. It is solved numerically that

$$
\begin{aligned}
&If\ r_t = 1, Then\\
&\gamma_{11r_t} = 0, \gamma_{12r_t} = 0, \gamma_{21r_t} = -0.0022,\\
&\gamma_{22r_t} = -7.1154 \times 10^{-4}, \gamma_{31r_t} = -7.7866 \times 10^{-4},\\
&\gamma_{32r_t} = -3.2993 \times 10^{-5},\\
&If\ r_t = 2, Then\\
&\gamma_{11r_t} = -0.0017, \gamma_{12r_t} = -0.0011, \gamma_{21r_t} = 0, \gamma_{22r_t} = 0,\\
&\gamma_{31r_t} = -6.0133 \times 10^{-5}, \gamma_{32r_t} = -1.9966 \times 10^{-5},\\
&If\ r_t = 3, Then\\
&\gamma_{11r_t} = -6.0133 \times 10^{-5}, \gamma_{12r_t} = -3.2993 \times 10^{-5},\\
&\gamma_{21r_t} = 0, \gamma_{22r_t} = 0,\\
&\gamma_{31r_t} = -0.0017, \gamma_{32r_t} = -0.0011,\\
&If\ r_t = 4, Then\\
&\gamma_{11r_t} = -7.7866 \times 10^{-4}, \gamma_{12r_t} = -1.9966 \times 10^{-5},\\
&\gamma_{21r_t} = -0.0022, \gamma_{22r_t} = -7.1154 \times 10^{-4},\\
&\gamma_{31r_t} = 0, \gamma_{32r_t} = 0.
\end{aligned}
$$

With the same settings as above, the feasible regions are shown in Figure 3. Set $a = 2$ and $b = 18$, we can obtain the controller gain matrices as

$$
\begin{aligned}
&If\ r_t = 1,\\
&K_{1r_t}(x_1) = [-1.9457x_1^2 - 0.2654x_1 - 2.4823,\\
&\qquad -0.3579x_1^2 - 0.0106x_1 + 4.1872],\\
&K_{2r_t}(x_1) = [-0.6603x_1^2 - 0.1432x_1 - 1.8275,\\
&\qquad -0.0854x_1^2 - 0.0739x_1 - 1.6914],\\
&If\ r_t = 2,\\
&K_{1r_t}(x_1) = [-0.4822x_1^2 + 0.0261x_1 - 0.3494,\\
&\qquad -0.0955x_1^2 + 0.0773x_1 + 0.7128],\\
&K_{2r_t}(x_1) = [-0.4535x_1^2 + 0.0321x_1 - 0.2784,\\
&\qquad -0.0529x_1^2 - 0.2017x_1 - 2.1793],\\
&If\ r_t = 3,\\
&K_{1r_t}(x_1) = [-0.3809x_1^2 + 0.0437x_1 - 0.0773,\\
&\qquad -0.0513x_1^2 - 0.1880x_1 - 3.4344],\\
&K_{2r_t}(x_1) = [0.0778x_1^2 + 0.0144x_1 - 0.2700,\\
&\qquad 0.0148x_1^2 + 0.0959x_1 + 2.1508],
\end{aligned}
$$

$$
\begin{aligned}
&If\ r_t = 4,\\
K_{1r_t}(x_1) &= [-0.0505x_1^2 + 0.0296x_1 - 0.0259,\\
&\quad -0.0005x_1^2 + 0.0028x_1 + 0.6512],\\
K_{2r_t}(x_1) &= [-0.0227x_1^2 + 0.0280x_1 + 0.0494,\\
&\quad -0.0027x_1^2 + 0.0001x_1 + 0.5836],
\end{aligned}
$$

and the Lyapunov matrix is $Q(x) = \begin{bmatrix} 0.6733 & -0.00403 \\ -0.00403 & 0.02326 \end{bmatrix}$.

According to the state feedback controller in (2), the closed-loop state responses under $x(0) = [-4, 3]^T$ or $x(0) = [2, -1]^T$ are shown in Figure 4. It can be seen from Figures 2 and 3 that larger feasible regions can be produced by using the switched fuzzy controllers.

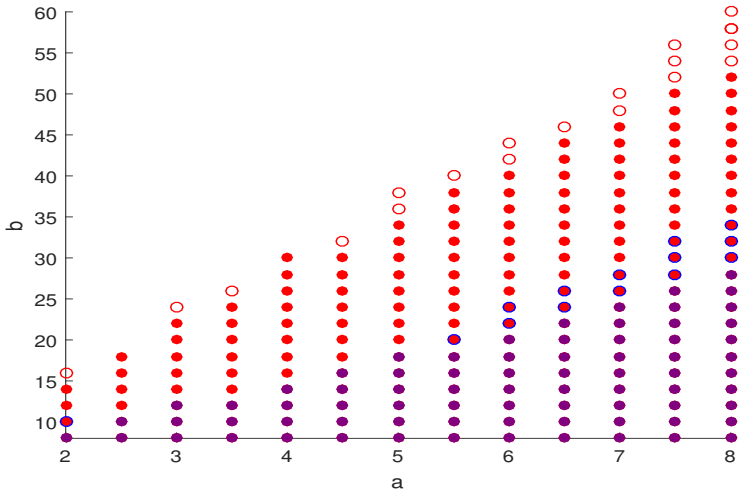



**Figure 2.** Stabilization regions with $Y_{jr_t}(x_1)$ of degrees 0 and 2 indicated by red "•" and "○" symbols, respectively. The feasible regions solved by the method in [18] are shown by blue "○" symbols. 'The purple "•" symbols show the feasible regions of the methods of [2,18] and the proposed method. The membership functions are sampled at $x_1 = \{-10, -9, \ldots, 9, 10\}$.

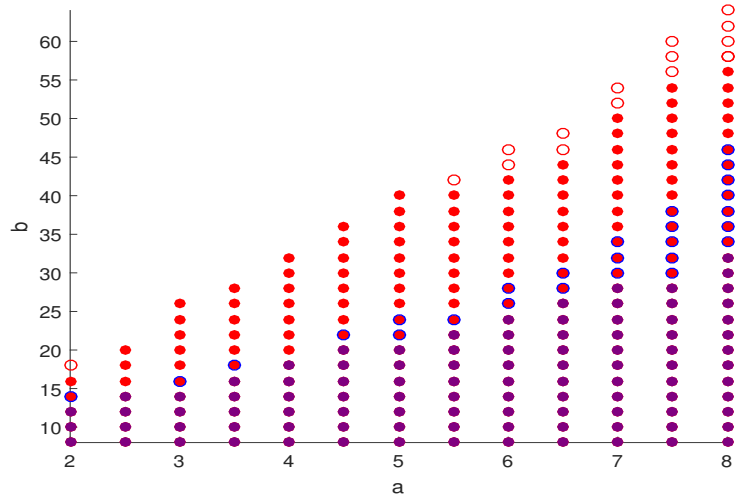
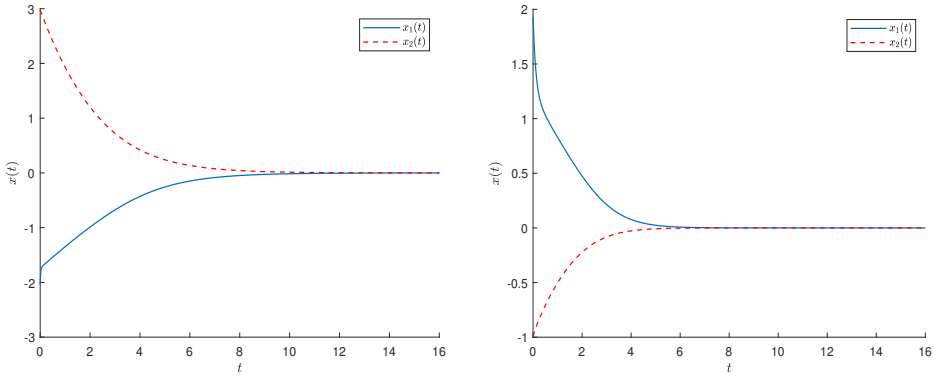



**Figure 3.** Stabilization regions with $Y_{jr_t}(x_1)$ of degrees 0 and 2 indicated by red "•" and "○" symbols, respectively. The feasible regions solved by the method in [18] are shown by blue "○" symbols. The purple "•" symbols show the feasible regions of the methods of [2,18] and the proposed method. The membership functions are sampled at $x_1 = \{-10, -9.5, \ldots, 9.5, 10\}$.




(**a**) initial value $[-4, 3]^T$ (**b**) initial value $[2, -1]^T$

**Figure 4.** The closed−loop state response of Example 1.

#### 4.1.1. Applicability Analysis

To demonstrate the applicability of the proposed method, we conduct the following additional tests on Example 1.

We test the closed-loop system under three different initial conditions: $x(0) = [-4, 3]^T$, $x(0) = [2, -1]^T$, and $x(0) = [-1, 5]^T$. All initial conditions converge to the origin, confirming that the region of attraction covers the feasible set identified by the SOS conditions.

We test with $q = 2, 3, 4$ subspaces for the same system. The feasible region enlarges monotonically with $q$, but with diminishing returns for $q > 4$. This demonstrates that increasing the number of subspaces reduces conservatism, at the cost of more SOS conditions to solve.

We test with $\deg(Y_{jr_t}) = 0, 2, 4$. Higher degrees enlarge the feasible region at the cost of longer computation time (2.37 s, 5.14 s, and 12.63 s, respectively).

#### 4.1.2. Comparative Studies

To quantitatively evaluate the conservatism reduction, we compare the feasible stabilization regions obtained by different methods for Example 1. The results are summarized in Table 1.

**Table 1.** Comparison of feasible stabilization regions for Example 1.

| Method | Feasible Area | Enlargement |
|---|---|---|
| Standard PDC [2] | 156.3 | — |
| Non-switched PFMB [18] | 193.7 | 23.9% |
| Proposed (Theorem 1) | 265.8 | 70.1% |

The proposed switched fuzzy controller achieves a 37.2% larger feasible region compared to the non-switched PFMB controller in [18] and a 70.1% enlargement compared to the standard PDC approach with quadratic Lyapunov function. This demonstrates that both the switched control scheme and the new relaxation technique contribute to conservatism reduction. For Example 2, the non-switched SOF controller in [29] cannot stabilize the system, while the proposed switched SOF controller (Theorem 2) successfully achieves stabilization, further demonstrating the necessity and effectiveness of the switching mechanism.

#### 4.1.3. Discussion of Simulation Results

The simulation results warrant further discussion regarding their control-theoretic implications. In Example 1, the larger feasible region (Figures 2 and 3) directly corresponds to a wider range of system parameters $(a, b)$ for which stabilization is achievable, meaning

the proposed method can handle more severely nonlinear systems. The switching behavior between subspaces can be interpreted as the controller adapting its gain structure to match the local nonlinearity characteristics in each operating region—when the system state moves from one subspace to another, the controller switches to a different gain matrix that is optimized for the local dynamics. In Example 2, the SOF controller achieves stabilization without requiring full state measurement, which is critical for practical applications where velocity states may be unmeasurable. The relationship between feasible region enlargement and conservatism reduction is as follows: a larger feasible region means that the SOS conditions are less conservative, as they certify stability for a broader class of system parameters.

### *4.2. Example 2*

Consider the PFMB system (1) with two local subsystems, and parameters

$$
\begin{aligned}
&If\ r_t = 1,\ then\\
&Y_{1r_t} = \begin{bmatrix} -0.06736x_1^2 + 0.01169x_1 - 16.19 & 0.001057x_1^2 + 0.6242x_1 + 6.486 \\ 0.0002298x_1^2 - 0.7266x_1 - 5.445 & 0.01749x_1^2 + 0.414x_1 - 9.013 \\ & -4.706e-6x_1^2 + 0.0003176x_1 - 0.04576 \\ & 6.03e-5x_1^2 - 0.002388x_1 - 0.1152 \end{bmatrix},\\
&Y_{2r_t} = \begin{bmatrix} -0.6333x_1^2 - 0.2631x_1 - 17.73 & 0.004037x_1^2 - 0.4657x_1 - 15.18 \\ -8.248e-5x_1^2 + 0.01459x_1 + 1.753 & -0.02368x_1^2 + 0.03726x_1 - 29.52 \\ & 1.979e-5x_1^2 + 0.005268x_1 - 0.09425 \\ & 3.39e-6x_1^2 + 2.957e-5x_1 - 0.007851 \end{bmatrix},\\
&If\ r_t = 2,\ then\\
&Y_{1r_t} = \begin{bmatrix} -0.02229x_1^2 - 0.001206x_1 - 19.78 & 0.0001102x_1^2 - 0.01097x_1 + 8.801 \\ 0.0004537x_1^2 + 1.643x_1 - 4.641 & -0.09425x_1^2 - 0.5392x_1 - 13.88 \\ & 1.557e-6x_1^2 - 0.001453x_1 - 0.01686 \\ & 5.334e-5x_1^2 + 0.003346x_1 + 0.2452 \end{bmatrix},\\
&Y_{2r_t} = \begin{bmatrix} 0.5404x_1^2 + 0.2583x_1 - 15.57 & -0.003185x_1^2 + 0.9486x_1 + 5.729 \\ 5.703e-5x_1^2 + 0.401x_1 - 2.339 & -0.05216x_1^2 - 0.09299x_1 - 5.416 \\ & -2.326e-5x_1^2 - 0.00651x_1 + 0.08099 \\ & 7.845e-6x_1^2 + 0.0004064x_1 + 0.01363 \end{bmatrix},
\end{aligned}
\tag{17}
$$

$$
\begin{aligned}
&If\ r_t = 1,\ then\\
&Z_{1r_t} = \begin{bmatrix} 0.1116x_1^2 - 0.1377x_1 + 18.16 & 0.00931x_1^2 - 1.421x_1 + 0.1953 \\ 0.0884x_1^2 + 0.08235x_1 - 0.04865 & 0.3186x_1^2 + 0.0772x_1 + 8.093 \\ -0.000858x_1^2 - 0.04331x_1 - 0.006373 & 0.0002608x_1^2 + 0.03488x_1 + 0.01869 \\ & 0.0003253x_1^2 - 0.02779x_1 - 0.09374 \\ & -0.0003382x_1^2 + 0.02823x_1 + 0.07359 \\ & 0.0002553x_1^2 - 8.589e-5x_1 + 0.09313 \end{bmatrix},
\end{aligned}
$$

$$Z_{2r_t} = \begin{bmatrix} 0.5377x_1^2 + 0.054x_1 + 18.73 & -0.2004x_1^2 + 1.197x_1 - 0.5145 \\ 0.04367x_1^2 + 0.04323x_1 + 0.6851 & 0.1555x_1^2 - 0.1376x_1 + 7.444 \\ -0.002735x_1^2 - 0.08312x_1 - 0.01306 & 0.001383x_1^2 + 0.01622x_1 - 0.03194 \end{bmatrix}$$
$$\begin{bmatrix} 0.0004616x_1^2 - 0.07548x_1 - 0.153 \\ -0.001359x_1^2 + 0.01647x_1 + 0.1301 \\ -1.987e-5x_1^2 + 7.96e-5x_1 + 0.01187 \end{bmatrix},$$

*If* $r_t = 2$, *then*

$$Z_{1r_t} = \begin{bmatrix} 0.05892x_1^2 + 0.03117x_1 + 19.69 & 0.007422x_1^2 + 0.3361x_1 + 0.123 \\ -0.04034x_1^2 + 0.08879x_1 - 0.3086 & 0.7441x_1^2 + 0.2391x_1 + 8.479 \\ -0.0001278x_1^2 - 0.01737x_1 + 0.02437 & 0.0003985x_1^2 + 0.02891x_1 - 0.05622 \end{bmatrix}$$
$$\begin{bmatrix} 2.703e-5x_1^2 - 0.0203x_1 - 0.1202 \\ 9.39e-5x_1^2 + 0.03033x_1 + 0.1189 \\ 3.928e-5x_1^2 - 4.985e-5x_1 + 0.1008 \end{bmatrix},$$

$$Z_{2r_t} = \begin{bmatrix} 0.4808x_1^2 - 0.04146x_1 + 18.03 & 0.09445x_1^2 - 0.4801x_1 + 0.4412 \\ 0.05021x_1^2 + 0.6635x_1 + 0.1384 & -0.1194x_1^2 - 0.3865x_1 + 8.301 \\ -0.001873x_1^2 - 0.08773x_1 + 7.961e-6 & 0.003116x_1^2 + 0.02585x_1 + 0.01516 \end{bmatrix}$$
$$\begin{bmatrix} 0.0002934x_1^2 - 0.07297x_1 - 0.1981 \\ -0.0004827x_1^2 + 0.01534x_1 + 0.1857 \\ 1.33e-6x_1^2 + 0.0002177x_1 + 0.01251 \end{bmatrix} \quad (18)$$

$$A_1(x_1) = \begin{bmatrix} 0.18 - 0.08x_1 & 1 - x_1 & 0.01 \\ 0.26 - 0.03x_1 & 0.59 - 0.12x_1 & -7.29 - 1.82x_1 \\ -0.01 & 0.01 & -2.85 \end{bmatrix},$$
$$A_2(x_1) = \begin{bmatrix} 4.35 + 0.11x_1 & -5x_1 & 0.002 \\ -5x_1 & 0.12 + 2.25x_1 & -4.64 + 0.72x_1 \\ 0.01 & 0.35 & 0.05 \end{bmatrix},$$

$$B_1(x_1) = \begin{bmatrix} 1 + 0.06x_1^2 & 0 \\ 0 & 1 + 1.35x_1 + 2.33x_1^2 \\ 0 & -0.5 \end{bmatrix},$$
$$B_2(x_1) = \begin{bmatrix} 8 + 2.35x_1^2 & 0 \\ 0 & 8 - 0.62x_1 + 0.56x_1^2 \\ 0 & -0.5 \end{bmatrix},$$
$$C_1(x_1) = C_2(x_1) = \begin{bmatrix} 1 & 0 & 0 \\ 0 & 1 & 1 \end{bmatrix}.$$

The MFs of the system and the fuzzy controller are given as

$$\begin{aligned} w_1(x_1) &= \exp(-\frac{x_1^2}{2 \times 0.5^2}), \\ w_2(x_1) &= 1 - w_1(x_1). \end{aligned}$$

It is shown in Figure 5 that the operating space $x_1$ of MFs is partitioned into two subspaces as $(-\infty, -0.5887] \cup [0.5887, +\infty)$, and $[-0.5887, 0.5887]$. The scalars $\gamma_{ijr_t}$ are solved as

$$
\begin{aligned}
&If\ r_t = 1,\ Then\\
&\gamma_{11r_t} = -0.0343,\ \gamma_{12r_t} = -0.0319,\\
&\gamma_{21r_t} = -0.0318,\ \gamma_{22r_t} = -0.0335,\\
&If\ r_t = 1,\ Then\\
&\gamma_{11r_t} = 0,\ \gamma_{12r_t} = -0.0707,\\
&\gamma_{21r_t} = -0.0707,\ \gamma_{22r_t} = -0.0414.
\end{aligned}
$$

If the control scheme in [29] reduces to the SOF control problem, the above system cannot be directly stabilized. By Theorem 2, the controller gains are solved as in (17) and (18), and the polynomial Lyapunov matrix is $Q(x) = \begin{bmatrix} 19.81 & 0.03127 & -0.1355 \\ 0.03127 & 10.35 & -1.742 \\ -0.1355 & -1.742 & 1.789 \end{bmatrix}$.

With the initial values of the states $x(0) = [2\ -1\ 1]^T$, the simulation result and the switching modes of the closed-loop system can be obtained and shown in Figure 6. Figure 7 shows the state response of the open-loop system.

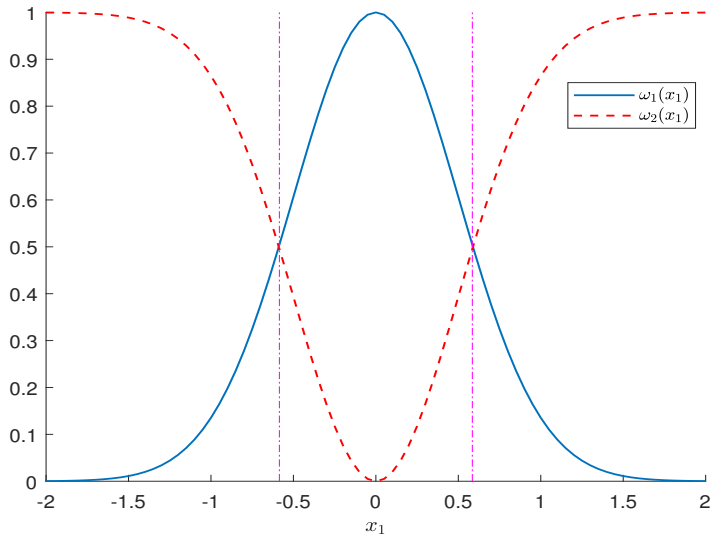
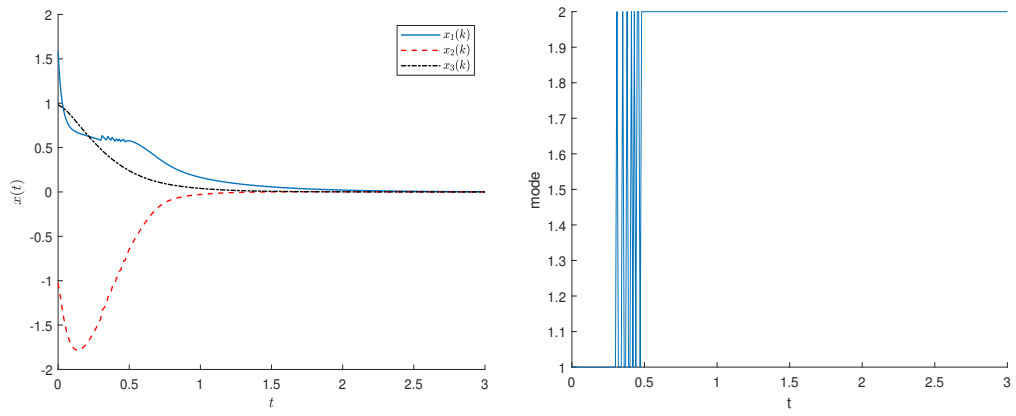



**Figure 5.** Membership function partition of Example 2.




(**a**) The closed-loop state response (**b**) The switching modes

**Figure 6.** The simulation results of Example 2.

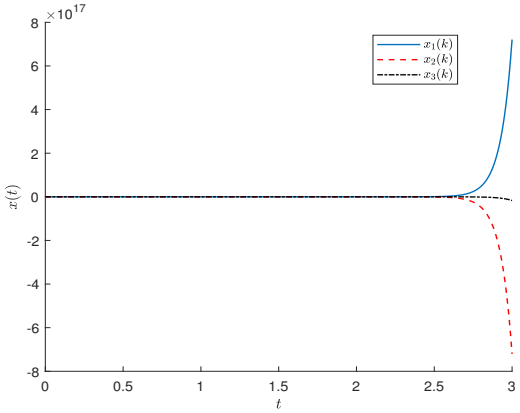



**Figure 7.** The open−loop state response of Example 2.

## 5. Conclusions

In this paper, we focused on the control problem for PFMB systems. We designed a switched state feedback and static output feedback controller via membership function partition. Then, by employing the piecewise-linear MF technique and a new relaxation method, a controller design was proposed in the form of SOS to guarantee the closed-loop systems to be asymptotically stable. Simulation results were given to demonstrate the validity and advantage of the presented method.

Several limitations of the proposed method should be noted. First, the computational complexity of SOS programming limits scalability to high-dimensional systems ($n > 5$) or high polynomial degrees ($d > 4$), as the SDP problem size grows rapidly. Second, the partition selection is not automated and currently relies on heuristic guidelines based on MF characteristics. Third, the method assumes exact knowledge of the polynomial system matrices, which may not hold in practice where model uncertainties exist.

The proposed framework has potential applications in robotic manipulators with polynomial dynamics, power systems with nonlinear loads, and chemical process control where T-S/PFMB models are commonly employed.

Future research directions include (i) extension to uncertain PFMB systems with polytopic or norm-bounded uncertainties, where robust stabilization conditions can be derived by incorporating uncertainty bounds into the SOS framework; (ii) incorporation of time delays and sampled-data control, which are common in networked control systems; (iii) automated partition optimization using machine learning or optimization-based methods to reduce the reliance on heuristic partition selection; (iv) extension to $H_\infty$ performance and robust control design for PFMB systems with external disturbances; and (v) development of event-triggered switching mechanisms to reduce communication burden in networked implementations.

**Author Contributions:** Conceptualization, L.G.; Methodology, L.G.; Software, M.H.; Validation, M.H.; Investigation, L.G.; Resources, L.G.; Writing—original draft, M.H.; Supervision, L.G.; writing-review, M.H. and L.G.; editing, L.G.; Funding acquisition, L.G. All authors have read and agreed to the published version of the manuscript.

**Funding:** This work was supported in part by the opening Foundation of Jiangsu Province Engineering Research Center of Smart Poultry Farming and Intelligent Equipment.

**Data Availability Statement:** Data are contained within the article.

**Conflicts of Interest:** The authors declare no conflicts of interest.

## References


1. Takagi, T.; Sugeno, M. Fuzzy identification of systems and its applications to modeling and control. *IEEE Trans. Syst. Man Cybern.* **1985**, *15*, 116–132. [CrossRef]
2. Tanaka, T.; Wang, H.O. *Fuzzy Control Systems Design and Analysis: A Linear Matrix Inequality Approach*; Wiley: New York, NY, USA, 2001.
3. Li, C.-X.; Wang, W.; Zeng, H.-B.; Zhang, X.-M. Novel stability and stabilization criteria for T-S fuzzy systems with time-varying delay based on fuzzy line integral. *Commun. Nonlinear Sci. Numer. Simul.* **2026**, *156*, 109663. [CrossRef]
4. Chen, J.; Lin, C.; Chen, B.; Wang, Q.-G. Regularization and stabilization for rectangular T-S fuzzy discrete-time systems with time delay. *IEEE Trans. Syst. Man Cybern. Syst.* **2019**, *49*, 833–842. [CrossRef]
5. Chang, X.-H.; Yang, G.-H. Nonfragile $H_\infty$ filtering of continuous-time fuzzy systems. *IEEE Trans. Signal Process.* **2011**, *59*, 1528–1538. [CrossRef]
6. Samidurai, R.; Yazhini, M.; Punitha, P.; Udhayakumar, R. LMI based non-fragile sample data control of fractional order T-S fuzzy complex valued neural networks with event triggered mechanism. *Inf. Sci.* **2026**, *741*, 123288. [CrossRef]
7. Liu, J.; Wei, L.; Cao, J.; Fei, S. Hybrid-driven $H_\infty$ filter design for T-S fuzzy systems with quantization. *Nonlinear Anal. Hybrid Syst.* **2019**, *31*, 135–152. [CrossRef]
8. Li, J.; Zhao, Y.; Feng, Z.; Park, M. Reachable set estimation and dissipativity for discrete-time T-S fuzzy singular systems with time-varying delays. *Nonlinear Anal. Hybrid Syst.* **2019**, *31*, 166–179. [CrossRef]
9. Kim, S.H. Enhanced relaxation-based local stabilization of T-S fuzzy systems: Achieving a simultaneous reduction in conservatism and complexity. *Results Control Optim.* **2026**, *22*, 100660. [CrossRef]
10. Ying, H.; Liu, S.; Shi, K.; Zhong, S.; Zhou, K. Delay-derivative/distribution dependent stability and stabilization criteria for T-S fuzzy systems with two additive stochastic time-varying delays. *Fuzzy Sets Syst.* **2026**, *533*, 109821. [CrossRef]
11. Feng, G. *Analysis and Synthesis of Fuzzy Control Systems—A Model Based Approach*; CRC: Boca Raton, FL, USA, 2010.
12. Bao, Z.; Li, X.; Shan, Y.; Wang, X.; Mehran, K.; Lam, H.K. Relaxed positivity, $\eta$-exponential stabilization and $l1$-gain performance of polynomial discrete-time fuzzy system with time-delay and external disturbance. *Fuzzy Sets Syst.* **2025**, *502*, 109221. [CrossRef]
13. Liu, X.; Zhang, Q. New approaches to $H_\infty$ controller designs based on fuzzy observers for Takagi-Sugeno fuzzy systems via LMI. *Automatica* **2003**, *39*, 1571–1582. [CrossRef]
14. Zhao, Y.-D.; Yu, H.-Y.; Ai, Z.; Cao, Y.; Zhang, B.-L. Fuzzy disturbance observer-based sampled-data fuzzy recoil control with memory for deepwater drilling riser systems. *Ocean. Eng.* **2025**, *342*, 123041. [CrossRef]
15. Tanaka, K.; Ohtake, H.; Seo, T.; Tanaka, M.; Wang, H.O. Polynomial fuzzy observer designs: A sum-of-squares approach. *IEEE Trans. Syst. Man Cybern. B Cybern.* **2012**, *42*, 1330–1342. [CrossRef]
16. Qiu, J.; Feng, G.; Yang, J. A new design of delay-dependent robust $H_\infty$ filtering for discrete-time T-S fuzzy systems with time-varying delay. *IEEE Trans. Fuzzy Syst.* **2009**, *17*, 1044–1058. [CrossRef]
17. Lam, H.K.; Narimani, M. Stability analysis and performance design for fuzzy-model-based control system under imperfect premise matching. *IEEE Trans. Fuzzy Syst.* **2009**, *17*, 949–961. [CrossRef]
18. Lam, H.K. Polynomial fuzzy-model-based control systems-stability analysis via piecewise-linear membership functions. *IEEE Trans. Fuzzy Syst.* **2011**, *19*, 588–593. [CrossRef]
19. Tu, W. Membership function-dependent robust sliding mode fault-tolerant control for T-S fuzzy systems with disturbances: A preset sliding band scheme. *Fuzzy Sets Syst.* **2026**, *533*, 109817. [CrossRef]
20. Zhu, C.; Sun, H.; Yang, J.; Hou, L.; Yang, D. Fuzzy dynamic adaptive event-triggered anti-disturbance control of fuzzy singularly perturbed systems via membership function-dependent $H_\infty$ performance. *Commun. Nonlinear Sci. Numer. Simul.* **2025**, *151*, 109007. [CrossRef]
21. Lam, H.K.; Li, H. Output-feedback tracking control for polynomial fuzzy-model-based control systems. *IEEE Trans. Ind. Electron.* **2013**, *60*, 5830–5840. [CrossRef]
22. Lam, H.K.; Lo, J.C. Output regulation of polynomial-fuzzy-model-based control systems. *IEEE Trans. Fuzzy Syst.* **2013**, *21*, 262–274. [CrossRef]
23. Lam, H.K. *Polynomial Fuzzy Model-Based Control Systems*; Springer: Berlin/Heidelberg, Germany, 2016.
24. Wang, L.; Zheng, B.; Xie, X.; Lam, H.-K. New Stability Criterion for Positive Impulsive Fuzzy Systems by Applying Polynomial Impulse-Time-Dependent Method. *IEEE Trans. Cybern.* **2024**, *54*, 5473–5482. [CrossRef] [PubMed]
25. Wang, Z.; Han, M.; Han, Y.; Guo, G.; Wang, Z. Improvement of controller design for positive polynomial fuzzy systems based on symbolic analysis and optimization of reduced-Order parameters of interval type-2 membership functions. *Fuzzy Sets Syst.* **2026**, *533*, 109836. [CrossRef]
26. Meng, A.; Lam, H.-K.; Liu, F.; Yang, Y. Filter Design for Positive T–S Fuzzy Continuous-Time Systems with Time Delay Using Piecewise-Linear Membership Functions. *IEEE Trans. Fuzzy Syst.* **2021**, *29*, 2521–2531. [CrossRef]
27. Lacerda, M.J.; Peixoto, M.L.C. Static output-feedback control for uncertain systems under input saturation and persistent disturbance. *Automatica* **2026**, *188*, 112943. [CrossRef]

28. Yang, Z.; Zhang, J. Reliability-guaranteed static output feedback control for linear systems with stochastic parametric uncertainty. *Syst. Control Lett.* **2025**, *205*, 106258. [CrossRef]
29. Lam, H.K. Stabilization of nonlinear systems using sampled-data output-feedback fuzzy controller based on polynomial-fuzzy-model-based control approach. *IEEE Trans. Syst. Man Cybern. B Cybern.* **2012**, *42*, 258–267. [CrossRef] [PubMed]
30. Liberzon, D. *Switching in Systems and Control*; Birkhauser: Berlin, Germany, 2003.
31. Liu, Q.; Zhao, J. Switched adaptive observers design for a class of switched uncertain nonlinear systems. *Nonlinear Anal. Hybrid Syst.* **2020**, *36*, 100866. [CrossRef]
32. Yuan, S.; Sun, Y.; Ju, X.; Yang, X. New conditions for a class of T-S fuzzy stochastic switched systems and application to electric circuit analysis. *Commun. Nonlinear Sci. Numer. Simul.* **2026**, *161*, 110140. [CrossRef]
33. Quispe, M.; Chiotti, D.; Aguila, J.D.; Quino, G.; Alegria, E.J. Automatic pellet positioner with switched fuzzy-PD control for a smart shrimp feeder. *Smart Agric. Technol.* **2026**, *13*, 101863. [CrossRef]
34. Qiu, J.; Feng, G.; Gao, H. Static-output-feedback $H_\infty$ control of continuous-time T-S fuzzy affine systems via piecewise Lyapunov functions. *IEEE Trans. Fuzzy Syst.* **2013**, *21*, 245–261. [CrossRef]
35. Song, G.; Lam, H.K.; Yang, X. Membership-function-dependent stability analysis of interval type-2 polynomial fuzzy-model-base control systems. *IET Control Theory Appl.* **2017**, *11*, 3156–3170. [CrossRef]
36. Wang, X.; Bao, Z.; Li, X.; Lam, H.-K.; Wang, Z. Dual Event-Triggered Polynomial Dynamic Output Control for Positive Fuzzy Systems via an IT2 Membership Function Relaxation Method. *IEEE Trans. Cybern.* **2026**, *56*, 3392–3405. [CrossRef]


**Disclaimer/Publisher's Note:** The statements, opinions and data contained in all publications are solely those of the individual author(s) and contributor(s) and not of MDPI and/or the editor(s). MDPI and/or the editor(s) disclaim responsibility for any injury to people or property resulting from any ideas, methods, instructions or products referred to in the content.